Chapter 1

Introduction

Most of the properties of simple metals can be accounted for by models where the conduction electrons are described by effectively free fermions, i.e. are described by a kinetic energy, an effective mass, and Pauli's principle. In some systems however, the Coulomb repulsion between electrons and the effects of exchange-correlations cannot be ignored. Once the interaction energy between electrons becomes comparable to their kinetic energy, the notion of *strongly correlated electron systems* (see [1] for an overview) has been established. Such systems exhibit a diversity of exotic and interesting properties, e.g. high-temperature superconductivity [2], heavy fermion behavior [3], and quantum magnetism [4].
Among the simplest models to describe itinerant electrons with strong correlations mediated via Coulomb repulsion is the Hubbard model

$$H = -t \sum_{\langle i,j\rangle,\sigma} \left(c^{\dagger}_{i,\sigma} c_{j,\sigma} + h.c. \right) + U \sum_{i} n_{i\uparrow} n_{i\downarrow}. \tag{1.1}$$

This Hamiltonian describes a hopping of electrons from one lattice site to another through creation $c^{\dagger}_{i,\sigma}$ and annihilation operators $c_{j,\sigma}$ with an additional Coulomb repulsion U between two electrons on the same site. At half filling and in the strong coupling limit $U >> t$, the Hubbard model can be reduced to the Heisenberg model

$$H = J \sum_{\langle i,j\rangle} \left[\Delta S^z_i S^z_j + \frac{1}{2} \left(S^+_i S^-_j + S^-_i S^+_j \right) \right] + g\mu_B B \sum_i S^z_i + D \sum_i (S^z_i)^2 \tag{1.2}$$

with $J = t^2/U$. While the kinetic and potential energies in real space are not of similar magnitude in the Heisenberg limit, this phenomenon still pertains to the spin space. In fact the exchange energy $\frac{J}{2} \left(S^+_i S^-_j + S^-_i S^+_j \right)$ is of identical magnitude as the Ising energy $J\Delta S^z_i S^z_j$ for the isotropic point $\Delta = 1$. These play a role similar to that of the

kinetic and potential energy, which becomes particularly evident in one dimension by a mapping to spinless fermions via the Jordan Wigner transformation $S_j^- = e^{-i\phi_j} a_j$, $S_j^+ = e^{i\phi_j} a_j^\dagger$, $S_j^z = a_j^\dagger a_j - \frac{1}{2} = n_j - \frac{1}{2}$. The phase $\phi_j = \pi \sum_{q=1}^{j-1} n_j$ counts the number of spinless fermions left of lattice site j to fulfill fermion commutation relations [5].

$$H = J \sum_{\langle i,j \rangle} \left[\Delta \left(n_i - \frac{1}{2} \right) \left(n_j - \frac{1}{2} \right) + \left(a_i^\dagger a_j + h.c. \right) \right] + g\mu_B B \sum_i \left(n_i - \frac{1}{2} \right) \quad (1.3)$$

In this picture, the coupling anisotropy Δ sets the ratio of kinetic to potential energy similar to the ratio U/t, and the the application of a magnetic field (Zeeman term) translates into the notion of a chemical potential, regulating the filling of the conduction band. Furthermore, the single-ion anisotropy D was introduced in eqn. (1.2) as a relevant model parameter for this thesis, owing to orbital quenching and spin-orbit coupling for spin $S \geq 1$ materials.

Despite its simplicity, the Heisenberg Hamiltonian is still a challenging subject for theory. Up to present times only static properties of the spin S=1/2 chain have been given exactly by Bethe in 1931 [6, 7] while it still proves to be challenging to calculate matrix elements of dynamic correlation functions for this particular system. Next to the well established Bethe ansatz [6] and field theoretical approaches (e.g. bosonization, conformal field theory, non-linear σ-model ([8–12]), *numerical* methods such as exact diagonalization (ED), lanczos diagonalization ([13, 14]), density matrix renormalization group (DMRG, [15] and ref. therein) and quantum Monte Carlo (QMC, [16] and ref. therein) play a key role in evaluating static and dynamic properties of quantum spin models.

The physics of the Heisenberg model, its critical behavior, and its ground state phases are influenced by the interplay of intrinsic properties, such as dimensionality, spin magnitude (i.e. quantum fluctuations), or magnetic frustration, and by extrinsic influences, such as magneto-elastic coupling or disorder. In particular the interplay of quantum fluctuations and reduced dimensions leads to many unusual effects. Focusing on one dimension, the absence of long range order has been established by Bethe's exact solution of the eigenvalue problem [6] for the spin S=1/2 chain. Field theoretical methods resulted in a critical exponent $\eta = 1$ of the algebraically decaying spin-spin correlation function $\langle S_i S_j \rangle \propto (-1)^{|i-j|} (\log |i-j|)^{1/2} / |i-j|^\eta$ (extensive review see [17]) and its low-energy properties are well described by those of a Luttinger liquid (LL) [9, 18], i.e. a description of bosonic collective excitations (spinons) with only two defining parameters: the spinon velocity v of the linear dispersion and the renormalized Luttinger parameter K which establishes interactions and governs the

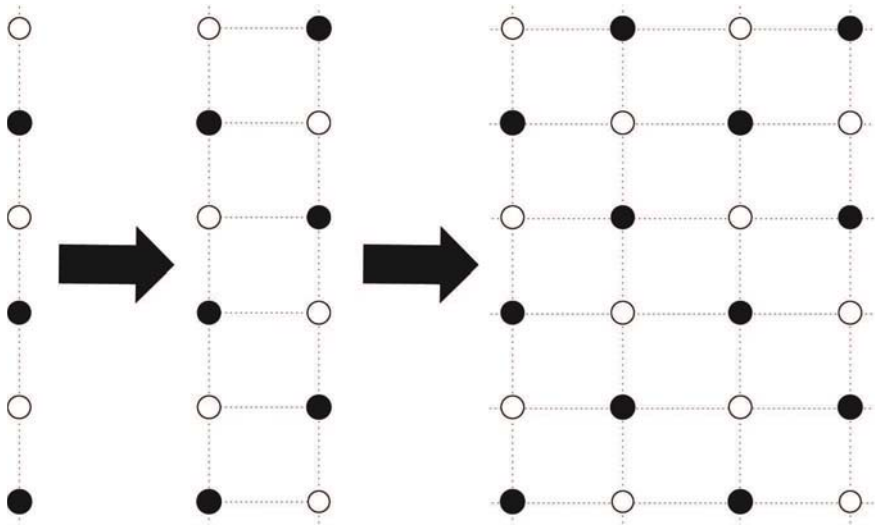

Figure 1.1: Illustration of the transition from a spin chain over a two-leg spin ladder to a two-dimensional plane. Empty, respectively closed circles stand for spins pointing up/down.

power-law decay of most correlation functions. With static properties well understood [7], dynamic and spin transport properties are however *still* subjects of discussions.

After establishing quantum criticality for the spin-1/2 chain, it came as a surprise when Haldane, employing the non-linear O(3) σ-model (NLσM) in a semi-classical large-spin approximation, suggested that only the half-integer spin chains are critical whereas all integer spin-chains have an energy gap Δ in the excitation spectrum [19]. As consequence, all thermodynamic properties activate exponentially and the spin-spin correlation function decays as $\langle S_i S_j \rangle \propto e^{-|i-j|/\xi}$ with a finite correlation length $\xi \propto 1/\Delta$[1].

The existence of a finite correlation length in the integer spin chains categorizes them as spin liquids, i.e. spin systems with no long range order and only short-range correlations. Another class of spin liquids relevant for my thesis is found in form of spin ladders [23], i.e. by increasing the dimensionality through linking chains into a two-dimensional alignment (see Fig. 1.1 for illustration). Such ladder systems alternate between spin liquid behaviour for even and critical behavior for odd number

[1] Note, that the ground state of the spin S=1 chain was found to have a hidden topological *string*-order [20–22].

of legs. A particularly interesting aspect of spin liquids in dimensions $d \geq 2$ is their field driven quantum phase transition into an ordered phase by condensing of the lowest magnon excitations (Bose-Einstein condensate). In the vicinity of the critical eld B_c, a universal scaling of the critical temperature T_c as function of magnetic field strength was predicted $T_c \propto (B - B_c)^\alpha$ with $\alpha = 3/2$ [24]. For $d = 1$, a breaking of the continuous XY-symmetry is permitted by Mermin-Wagner's theorem, therefore a critical temperature does not exist. However, in an already magnetized state there remains no conceptual difference in the low energy properties between spin ladders, integer and half-integer spin chains [25, 26]. Interestingly, this crossover into a Luttinger liquid is driven by *increasing* the magnetic field. For the spin S=1/2 chain it is observed upon *decreasing* the magnetic field through its critical value.

In my thesis, the main points of interest are (i) numerical methods and (ii) static and dynamic properties of spin systems in reduced dimensionality and in the vicinity of quantum critical points. The thesis is structured threefold. In the first part, the employed QMC method will be introduced. In a small introduction of the most common numerical methods, I will motivate our choice as QMC proves to be a very powerful and flexible tool, tailored for evaluation of large systems in any dimension down to essentially zero temperature. Its adjacent discussion features a small introduction to quantum Monte Carlo and systematically explains its implementation for the particular case of the stochastic series expansion (SSE). The latter provides a detailed discussion about measuring longitudinal and transverse imaginary time observables which, to the best of my knowledge, is still insufficiently documented in literature. As a consequence of results in imaginary time, two common analytic continuation algorithms will be introduced in section 2.5. Such continuations from imaginary to real axis are required to perform comparisons with experiments such as inelastic neutron scattering (INS) or nuclear magnetic resonance (NMR). After the methodical aspect of this thesis, results will be presented in chapter 3 and 4. While the first part of my results (chapter 3) features exclusively static quantities of low-dimensional spin systems, the second part (chapter 4) focuses on dynamic properties of the spin S=1/2 and S=1 chain with a short introduction to spin transport of the spin S=1/2 system.

In further detail, chapter 3 is divided threefold: the first section 3.1 deals with thermodynamic properties of quantum spin S chains with $S \in \{1/2, 1, 3/2, 2, 5/2\}$. By means of the static susceptibility we contrast the quantum spin model with a classical $S \to \infty$ limit by Fisher [27]. After a finite size analysis for all spin magnitudes in a temperature range $0.01 \leq T/J \leq 100$, we find that even for the largest evaluated spin S=5/2 there are considerable differences in terms of the maximum position and the

low temperature behavior compared to the $S \to \infty$ limit. Additionally, Padé-fits are given for the whole evaluated temperature region to allow for an analytical access to our numerical data. We evaluate our fit quality through a comparison to high-accuracy Bethe-ansatz data in the case of spin S=1/2 and suggest improvements of commonly used fit formulas available in literature for all evaluated spin magnitudes.

In section 3.2, we analyze thermodynamic properties of a spin S=1 two-leg ladder as function of rung/leg coupling and single-ion anisotropy. Such a ladder system is unique in many regards: first of all we know that even-leg spin S=1/2 ladders show spin liquid behavior and naturally we expect the same for a spin S=1 ladder system. In the coupling limits of zero inter-chain and zero intra-chain coupling, we find two uncoupled Haldane chains, respectively uncoupled dimers – both systems which display a strong spin gap. In the region of intermediate coupling however, Todo *et al.* showed a weakening of the gap by nearly two orders of magnitude. At this point we utilize QMC in the thermodynamic limit to show that for intermediate coupling ratios and an additional small easy-plane anisotropy, the system seems to become *gapless*. This results in finite susceptibilities even at lowest elevated temperatures $T/J = 0.001$ and the low-temperature magnetization profile loses the typical step-structure of a spin ladder. Additionally we compare our results to susceptibility and magnetization measurements of Mennerich *et al.* [28] on a Ni(II) based spin S=1 ladder material in order to elaborate on its coupling constants. Ultimately, all comparisons point at weakly coupled dimers for this system with a small easy-plane anisotropy – too small to lift the gap.

In the last section of chapter 3, we study an essentially zero-dimensional [3 × 3]-grid system with large spin S=5/2, motivated by susceptibility and magnetization measurements on a molecular magnet based on Mn(II) ions [29]. Such molecular magnet with such a large effective magnetic moment may have many technically interesting applications, such as e.g. storage device for conventional bits due to the large relaxation time of the magnetization (one month at 2K) or as basis for quantum computing if the tunnel barrier of the Néel vector is not too large. Interestingly, the system exceeds the computational limits of exact diagonalization despite its small size, which means exact theoretical results are largely absent. Among the observables we compute are susceptibility, magnetization and (staggered) static structure factor as function of temperature, center spin coupling, magnetic field and single-ion anisotropy. As far as the temperature and center-spin coupling variation is concerned, we find very low impact on the form of the susceptibility. High- as well as low temperatures show solely Curie behavior with very marginal variation in an intermediate temperature region $1 \leq T/J \leq 10$. Upon variation of the single- ion anisotropy however, strong

effects occur. For a small easy-plane anisotropy, the system aligns immediately in-plane, leading to an Ising-like total spin S=1/2 with clear fingerprints in the magnetization steps and (staggered) structure factor. Likewise we find an immediate aligning along the z-axis with the application of a small easy-axis anisotropy, leading to a total spin S=5/2 with clear indications given in the magnetization profile and (staggered) structure factor. Finally, with an extensive parameter study, we provide a very accurate description for the whole available temperature region $1K \leq T \leq 300$K to the experimental susceptibility of the Mn-[3×3] grid and our magnetization profile qualitatively reflects magneto-torque measurements performed by O. Waldmann [30].

Chapter 4 is also divided threefold. In section 4.1 we study dynamic properties of the Heisenberg spin S=1/2 chain as function of temperature and magnetic field – a parameter-combination where theoretical results are lacking. Among our observables are longitudinal as well as the transverse structure factor for the Luttinger liquid regime $0 \leq B < B_c$ up to fields beyond the saturation field. We detail the field and temperature dependence of the incommensurate fermi vectors and clarify finite temperature q-dependence of the system at full polarization by a two-magnon excitation model. Additionally we analyze the $1/T_1$-relaxation rate and successfully compare it to experiments by H. Kühne *et al.* [31]. Their experiments and our numerical results strongly reflect the condensation of magnons upon *decreasing* the field through the saturation field B_c in a diverging relaxation rate for $T \to 0$. Interestingly, the maximum of the $1/T_1$-relaxation rate at finite temperatures is found *below* the critical field for both, theory and experiment.
The same critical behavior of a level-crossing magnon dispersion has mostly been looked at upon *increasing* the magnetic field for gapped systems such as Haldane chain or spin ladder materials. With that in mind, we look at the dynamics of the Haldane system as function of temperature and magnetic field in section 4.2, which, in the case of $B = 0$, is fundamentally different from the dynamics of the spin S=1/2 chain. The Haldane dynamics are dominated by a sharp, gapped magnon dispersion while the spin S=1/2 system is known to consist of spinons spanning an energy continuum. However, upon increasing the field for the Haldane system, the spin gap closes and the system can be described by a Luttinger liquid again, resembling the dynamic properties of the spin S=1/2 system discussed earlier. In that regard, we look at the evolution of the transverse dynamic structure factor as function of field and temperature and discuss it for the gapped $0 \leq B \leq B_{c_1}$ and the LL regime $B_{c_1} \leq B \leq B_{c_2}$. Furthermore we extract the relaxation rate and show its exponential increase by populating the gap through heating, respectively upon approaching the first critical field at a fixed finite temperature. Both, section 4.1 as well as 4.2, close with a discussion of sum rules as a consistency check for our analytic continuations from the imaginary to the real axis.

This leads to section 4.3 (as follow-up to dynamic properties of the spins S=1/2 Heisenberg chain), dealing with transport properties of the isotropic spin S=1/2 Heisenberg chain, which has been under intense scrutiny since one decade without coherent results for the nature of the transport at the SU(2) symmetric point, e.g. ballistic or diffusive. Unfortunately our analytical continuations with the commonly assumed error of 10-20% are not sufficiently accurate to enter this discussion with reasonable arguments on the real axis. Very recently however, spin diffusion has been conjectured to governs the low-frequency spectrum of the regular conductivity which provides for an approximate expression of the Fourier transform of the retarded spin susceptibility [32]. This expression can be transformed to imaginary time, where our QMC results are *only* subject to statistical errors. With considerable numerical effort we show that our data is supporting a diffusive channel for the XXZ-model, which opens up the intriguing possibility of a finite temperature dynamical spin conductivity of the Heisenberg model which comprises both, a finite Drude weight and a regular part with a large mean free path at low temperatures.